

Intrinsic Mechanism of UV-C-Induced Inactivation of *Microcystis aeruginosa*: Impairment on Photosynthetic System

Jiazhao He · Huase Ou · Jiexiong Chen · Juan Liu · Dehua Lu

Received: 18 October 2015 / Accepted: 25 January 2016 / Published online: 13 February 2016
© Springer International Publishing Switzerland 2016

Abstract To investigate the intrinsic mechanism of UV-C-induced impairment on cyanobacterial photosynthetic system, a one-off UV-C irradiation and a subsequent 6-day cultivation of *Microcystis aeruginosa* were conducted. The pulse amplitude modulation fluorometry was used to determine the variations of chlorophyll-a and light-induced curve (LIC); furthermore, the low temperature (77 K) fluorescence technique was used to analyze the emission spectra of photosynthetic apparatus. For 4.6×10^6 cells mL^{-1} *M. aeruginosa* suspension, 0–280 mJ cm^{-2} UV-C irradiation induced an accumulation of chlorophyll-a; however, higher dosage ($>280 \text{ mJ cm}^{-2}$) UV-C resulted in a decline of chlorophyll-a during the subsequent cultivation. The results of 77-K spectra demonstrated that UV-C induced intracellular damages of phycobilisome, photosystem I, photosystem II, and thylakoid. The LIC results showed that UV-C suppressed two important photosynthetic strategies: state transition and non-photochemical quenching. Consequently, the UV-C-induced impairment of cyanobacterial photosynthetic system can be summarized as a three-step process: (1) degradation of

photosynthetic pigments, (2) decomposition of photosynthetic apparatus, and (3) inhibition of photoacclimation and photoprotection. These impairments resulted in a decline of cyanobacteria community. For 4.6×10^6 cells mL^{-1} cyanobacteria, 0–280 mJ cm^{-2} UV-C irradiation induced a decline-recovery procedure of *M. aeruginosa* cells, but 700–4200 mJ cm^{-2} UV-C irradiation caused a continuous decrease of cell density (from 4.5×10^6 cells mL^{-1} to 0) within 6-day cultivation. These results implied that, for a given biomass cyanobacteria community, there is an optimal UV-C dosage threshold to achieve complete inactivation.

Keywords UV-C · Photosynthesis · Inactivation · Cyanobacteria · *Microcystis aeruginosa*

1 Introduction

Cyanobacteria are essential parts in biosphere as the basic producers and important food sources for aqueous organisms (Parmar et al. 2011; Vaishampayan et al. 2001). However, cyanobacteria blooms frequently occurred as a result of eutrophication in lakes, reservoirs, rivers, and other drinking water sources (Briand et al. 2003; de Figueiredo et al. 2004), accompanied by several serious problems. First, some specific cyanobacteria (e.g., *Microcystis aeruginosa*) can produce cyanotoxins (e.g., microcystin-LR) those have low acute lethal doses ($10 \leq \text{LD}_{50} \leq 100 \text{ mg/kg}$) to human and livestock (Azevedo et al. 2001). Long-term low-dosage exposure ($<40 \mu\text{g L}^{-1}$) of the most toxic microcystin,

J. He · H. Ou (✉) · J. Liu · D. Lu
Guangzhou Key Laboratory of Environmental Exposure and Health, School of Environment, Jinan University, Room 446, The Second Science and Technology Building, Jinan University, 601 Huangpu Avenue West, Guangzhou 510632, People's Republic of China
e-mail: touhuase@jnu.edu.cn

J. Chen
Shantou Marine Plants Experiment Station, Chinese Academy of Sciences, Shantou 515041, China

microcystin-LR, has chronic toxicity on hepatocyte mitochondria of mice (Li et al. 2015). Second, water supply suffers from cyanobacterial taste and odor materials, e.g., geosmin and 2-methylisoborneol (Watson et al. 2008). Third, the residue and excretion released from rupturing cyanobacteria cells increase the natural organic matters in natural water bodies, and these materials are well-known precursors of disinfection by-products (Huang et al. 2009). Consequently, the harmless removal of cyanobacteria cells and their derived organic materials have become a tough issue in water treatment due to their heterogeneity and complexity.

In drinking water and wastewater treatments, ultraviolet light (UV) is a frequently used approach for the inactivation of bacteria (Zhou and Smith 2001). The investigation regarding to UV-induced damage of genetic system was performed excessively. However, cyanobacteria rely on an oxygenic photosynthetic system to perform photosynthetic energy conversion. This system is a highly developed organic structure, which includes: (1) a series of light harvesting pigments, such as chlorophyll(s) and phycocyanin (PC) (MacColl 1998) and (2) a number of photosynthetic apparatus, such as photosystem II (PS II), photosystem I (PS I) reaction centers and phycobilisomes (PBS) (Campbell et al. 1998). This system was proven to be sensitive to high-energy UV irradiation, such as UV-C (200–280 nm) and UV-B (280–320 nm). It was validated that UV-B stress had negative effects on photosynthesis (He and Hader 2002). Only a few researches focused on the UV-C-induced photosynthetic system impairment (Chen et al. 2012). However, the detailed mechanism and effect of UV-C on the photosynthetic systems of cyanobacteria was still unknown.

The studies of photosynthesis status have been facilitated by the introduction of chlorophyll fluorescence analysis. In practice, pulse amplitude modulation (PAM) fluorometry in conjunction with the low-temperature (77 K) fluorescence emission spectra was particularly successful. The light capture and electron transport in photosynthesis can be investigated by PAM, and the characteristic spectra of photosynthetic apparatus can be analyzed by the 77-K spectra. It was reported that PAM and 77-K spectra can provide an excellent representation of the PS II activity in cyanobacteria and a better identification of the physiological mechanism (Bailey and Grossman 2008; Campbell et al. 1998). Therefore, these two methods were expected to provide

useful information about the inactivation mechanism of cyanobacteria by UV-C irradiation.

In the current study, *M. aeruginosa* was selected as an indicative cyanobacterium, and the multiple analyses were used to investigate the performance of *M. aeruginosa* photosynthesis system after UV-C irradiation. The aims of this study were to (1) monitor the short-term (immediately) and long-term (6 days) effects of UV-C on photosynthesis and biomass and (2) investigate the mechanism of UV-C-induced impairment on photosynthetic pigments, apparatus, photoacclimation, and photoprotection capacities. The current study may provide useful information, from another perspective, to reveal the mechanisms in UV-C inactivation of cyanobacteria.

2 Experimental Section

2.1 Culture Condition of *M. aeruginosa* and Materials

A toxic strain of *M. aeruginosa* (FACHB-912) was purchased from the Institute of Hydrobiology, Chinese Academy of Sciences (Wuhan, China). This strain was cultivated by BG11 medium in 1-L glass conical flasks using an incubator (SPX-250B-G, Cany, China) at ~25 °C. The flasks were illuminated by tubular fluorescent lamps at ~30–40 $\mu\text{mol photons m}^{-2} \text{s}^{-1}$ under a CO₂-enriched atmosphere (at a concentration of 0.039 % by volume) with a 12-h diurnal cycle. The light intensity was measured by a submersible spherical micro quantum sensor (US-SQS/L, Walz, Germany). All of the solutions were prepared using ultrapure water (electrical resistivity: 18.2 M Ω) produced by a Milli-Q Advantage A10 system (Millipore, USA).

2.2 UV-C Irradiation and Cultivated Experiments

The *M. aeruginosa* cultivation was collected in logarithmic growth phase and diluted by BG11 medium to $\sim 4.6 \times 10^6$ cells mL⁻¹ (~ 0.8 μg chlorophyll-a mL⁻¹). The cell concentration was determined by a microscope (YS100, Nikon, Japan) using hemacytometer counting method and by a CytoSense flow cytometry (CytoBuoy, Netherlands). The suspension pH was pre-adjusted to 7.0 using a 5.0 mM phosphate-buffered solution. The UV irradiation experiments were conducted using a customized device, which was composed of a 1.5-L conical glass vessel, a thermostatic magnetic

stirrer, and a removable low-pressure mercury lamp (8 W, effective length 25 cm, surface light intensity $\sim 4.31 \text{ mW cm}^{-2}$, Philips, Holland). The illuminating intensity was 2.30 mW cm^{-2} . Detailed information about this device and the UV-C dosage calculation can be found in our previous study (Ou et al. 2011).

UV-C treatments were carried out in triplicate under $25 \pm 2 \text{ }^\circ\text{C}$. Prior to experiments, the UV lamp was turned on to warm up for 30 min. The one-off UV-C exposure experiments were carried out by spiking 1.3 L *M. aeruginosa* suspension into the reactor. At each designated UV-C irradiation dosage, 390 mL suspension was obtained. This suspension sample was divided into four parts: (1) 20 mL for PAM and flow cytometry analyses, (2) 20 mL for fluorescence emission spectra analysis, (3) 50 mL for transmission electron microscope (TEM) analysis, and (4) 300 mL for subsequent cultivation. The subsequent 6-day cultivation was conducted under the same condition mentioned in section 2.1. During cultivation, a 20-mL sample was obtained daily for PAM and flow cytometry analyses. Another 20-mL sample was harvested for the fluorescence emission spectra analyses every 2 days.

2.3 Analytical Methods

In order to obtain the mean chlorophyll-a concentration (MCC), the determinations of total chlorophyll-a concentration (TCC) and cell density (CD) were performed. The variation of CD was determined by the flow cytometry using the same method reported in the previous study (Ou et al. 2012). The in vivo TCC was measured using a PAM fluorometer (DUAL-PAM-100, Walz, Germany) (Lu et al. 2011). The MCC was calculated as:

$$MCC = \frac{TCC}{CD} \quad (1)$$

where MCC and TCC has the same unit of ng cell^{-1} , and CD has a unit of cell L^{-1} . All measurements using PAM were carried out in a stirred cuvette with 1-cm diameter under room temperature ($25 \pm 2 \text{ }^\circ\text{C}$).

After the determination of chlorophyll-a concentration, the measurements of light-induced curve (LIC) were also conducted using PAM (Ralph and Gademann 2005; White and Critchley 1999). The suspension was concentrated to $5\text{-}\mu\text{g}$ chlorophyll-a mL^{-1} and kept in dark for 5 min. The minimal fluorescence level (F_0) was determined by illuminating cells with a low, modulated light ($1 \text{ }\mu\text{mol photons m}^{-2} \text{ s}^{-1}$). Under

this condition, all photosynthesis reaction centers opened, and no measurable charge was induced. Thereafter, these cells were illuminated by a low-intensity white light ($60 \text{ }\mu\text{mol photons m}^{-2} \text{ s}^{-1}$) for ~ 1.5 min to obtain the first steady-state fluorescence level (F_s); then these cells were illuminated by a $600 \text{ }\mu\text{mol photons m}^{-2} \text{ s}^{-1}$ high-intensity white light for ~ 2 min to obtain the second steady-state fluorescence level (F_s'). Finally, the cells were shifted back to a low-intensity white light ($60 \text{ }\mu\text{mol photons m}^{-2} \text{ s}^{-1}$), and the third steady-state fluorescence level (F_s'') was measured.

The maximal fluorescence levels ($F_{m,d}$, F_m' , F_m'' , and F_m''') were measured by applying pulsed saturated white light which transiently closed all PS II centers in different steady-state fluorescence level periods. The fluorescence value in LIC has a relative unit (a.u.) (Boulay et al. 2008). In the current experiment, three parameters were calculated by the following equations:

$$\text{Level 1} \quad dF_s = F_s - F_0 \quad (2)$$

$$\text{Level 2} \quad dF_s = F_s' - F_s \quad (3)$$

$$dF_m' = F_m' - F_m'' \quad (4)$$

Level 1 dF_s and Level 2 dF_s are the level 1 and level 2 state transitions, respectively, and dF_m' is the non-photochemical quenching.

Fluorescence emission spectra at 288 K and 77 K were measured by a CARY Eclipse fluorescence spectrophotometer (Varian, USA). The excitation wavelengths (Ex) were set at 430 and 600 nm, and the emission wavelengths (Em) ranged from 620 to 800 nm with the sampling intervals of 1 nm. The slits for both excitation and emission were 10 nm with a scanning speed at 50 nm min^{-1} . The *M. aeruginosa* samples were concentrated to $5\text{-}\mu\text{g}$ chlorophyll-a mL^{-1} . The samples in NMR tubes (5-mm diameter) were quickly frozen to 77 K by an OptistatDN liquid nitrogen optical spectroscopy cryostat system (Oxford Instruments, UK) and then they were measured under constant 77 K condition. TEM was used to characterize the morphology. The detailed pre-treatments and measure processes of TEM can be found in the previous study (Ou et al. 2011).

2.4 Quantitative PCR

The coding gene expressions of *psbA* for PS II core protein D1 and *cpc* for PC were quantified using real-time quantitative polymerase chain reaction (RT qPCR). Detailed pre-treatment and analysis were followed the same procedure as Ref. (Yi et al. 2013). Transcriptions of *psbA* and *cpc* were determined using a CFX96 Real-Time PCR Detection Systems (BIO-RAD, USA).

3 Results

3.1 Variations of Photosynthetic Pigments

The TCC in suspension and the MCC in a single cell (calculated using Eq. 1) were used to represent the variation of pigment (Fig. 1). The data at 0 day were the values measured immediately after UV-C treatment, and the data at n d were the values measured after n d cultivation. At 0 day, the TCC slightly increased when the UV-C dosage increased (<1400 mJ cm^{-2}). TCC increased to $2240 \mu\text{g L}^{-1}$ when the UV-C dosage reached 1400 mJ cm^{-2} , and it decreased to $614 \mu\text{g L}^{-1}$ when UV-C dosage reached 4200 mJ cm^{-2} . Similar variation pattern was observed in MCC result at 0 day. In the 6-day cultivation, the TCC in control samples (0 mJ cm^{-2} UV-C) gradually increased from 857 to $1587 \mu\text{g L}^{-1}$, and the

MCC maintained in the range from $1.74 \times 10^{-4} \text{ ng cell}^{-1}$ to $1.86 \times 10^{-4} \text{ ng cell}^{-1}$. After 70 mJ cm^{-2} UV-C irradiation, the TCC gradually increased from 846 to $1339 \mu\text{g L}^{-1}$. The MCC initially increased from $1.84 \times 10^{-4} \text{ ng cell}^{-1}$ (0 day) to $2.10 \times 10^{-4} \text{ ng cell}^{-1}$ (3 days). It decreased to $1.82 \times 10^{-4} \text{ ng cell}^{-1}$ at 6 days. After 140 mJ cm^{-2} UV-C irradiation, the TCC and MCC initially increased from $872 \mu\text{g L}^{-1}$ to $1041 \mu\text{g L}^{-1}$ and from $1.90 \times 10^{-4} \text{ ng cell}^{-1}$ to $2.32 \times 10^{-4} \text{ ng cell}^{-1}$ during the first 3-day cultivation. In subsequent 3-day cultivation, TCC and MCC respectively decreased to $9.58 \times 10^{-4} \text{ ng cell}^{-1}$ and $1.93 \times 10^{-4} \text{ ng cell}^{-1}$. More significant initial increases of TCC and MCC were observed in the samples treated by 280 mJ cm^{-2} UV-C. Both TCC and MCC decreased to approximate 0 within 4 days after higher UV-C irradiation ($>280 \text{ mJ cm}^{-2}$).

3.2 Variations of Fluorescence Emission Spectra

In order to assess the impairment of UV-C on photosynthetic apparatus, 298 and 77-K fluorescence emission spectra were used to monitor the changes of PS II, PS I, and PBS after UV-C irradiation (Fig. 2). When samples were excited at 430 nm , the 298-K fluorescence emission spectra were characterized by a major band at 680 nm and a minor band at 720 nm (Fig. 2a). These bands related to in vivo chlorophyll-a in PS I and PS II, respectively (Kirilovsky 2007). It can be seen that these bands slightly

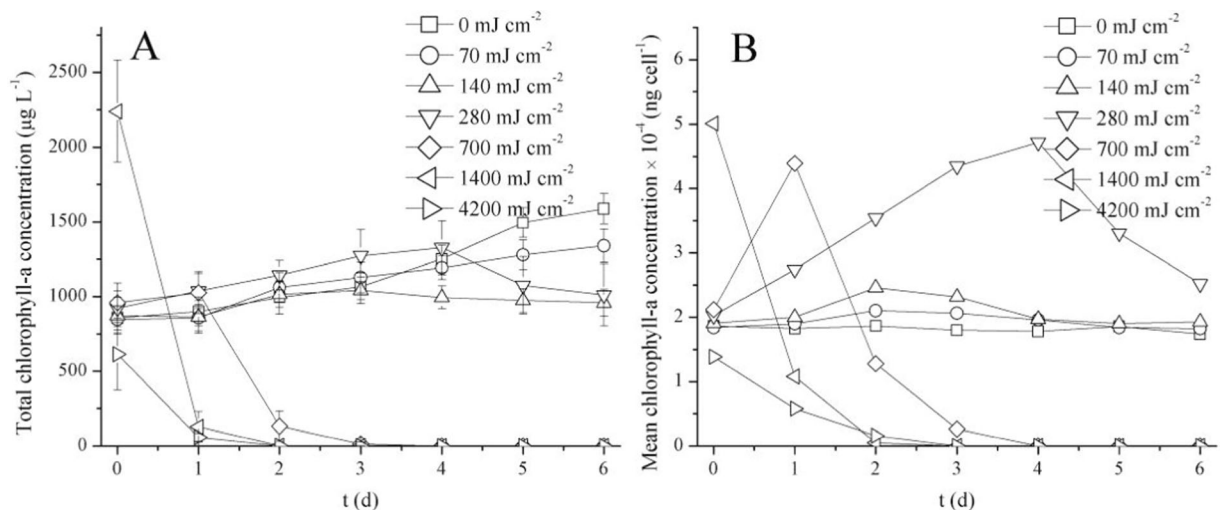


Fig. 1 Variation of chlorophyll-a concentration of *M. aeruginosa* in cultivation after UV-C irradiation. **a** Total in vivo chlorophyll-a concentration in suspension, **b** mean in vivo chlorophyll-a concentration in a single cell. UV-C intensity was 2.30 mW cm^{-2} . The 0 mJ cm^{-2} sample at 0 day was the control sample without UV-C

treatment. The other data at 0 day were the chlorophyll-a concentrations immediately after given dosages UV-C treatment. The data at n d were the values obtained after n d cultivation. The curve in Fig. 1a was the mean value of three replicates; error bars indicated the ± 1 standard deviation of each data set

decreased when UV-C dosage reached 280 mJ cm^{-2} and increased when UV-C reached 700 mJ cm^{-2} . Similar variation was observed in the result of 600-nm excitation, which related to PC in PBS (Fig. 2c).

Under 77-K condition, only the intrinsic molecule fluorescence spectra can be observed; thus, the 77-K fluorescence spectra were used to investigate the intrinsic variations of photosynthetic apparatus. When the control sample was excited at 430 nm, the 77-K fluorescence spectra showed bands at 685 and 695 nm, which related to the CP43 and CP47 chlorophyll antenna in PS II, respectively (Wilson et al. 2007). Another large band at 725 nm, which related to PS I chlorophyll, was observed (Fig. 2b). When the control sample was excited at 600 nm, the bands related

to PC (650 nm), allophycocyanin (APC, 660 nm), PS II (685 and 695 nm), and PS I (725 nm) were observed (Fig. 2d). Since the PS I in *M. aeruginosa* contained little PBS (Nield et al. 2003), a small emission band at 725 nm was observed. After 280 mJ cm^{-2} UV-C irradiation, all these bands decreased. When the UV-C dosage increased to 700 mJ cm^{-2} , these bands continued to decline.

The variations of 77-K fluorescence emission spectra of the cultivating samples are presented in Fig. 3. In the control samples, the emission spectra increased during 6-day cultivation, indicating a growth of cell community. In the 280-mJ cm^{-2} treated sample, the bands gradually decreased in the initial 4 days and slightly increased in subsequent 2-day cultivation (Fig. 3c, d), suggesting a

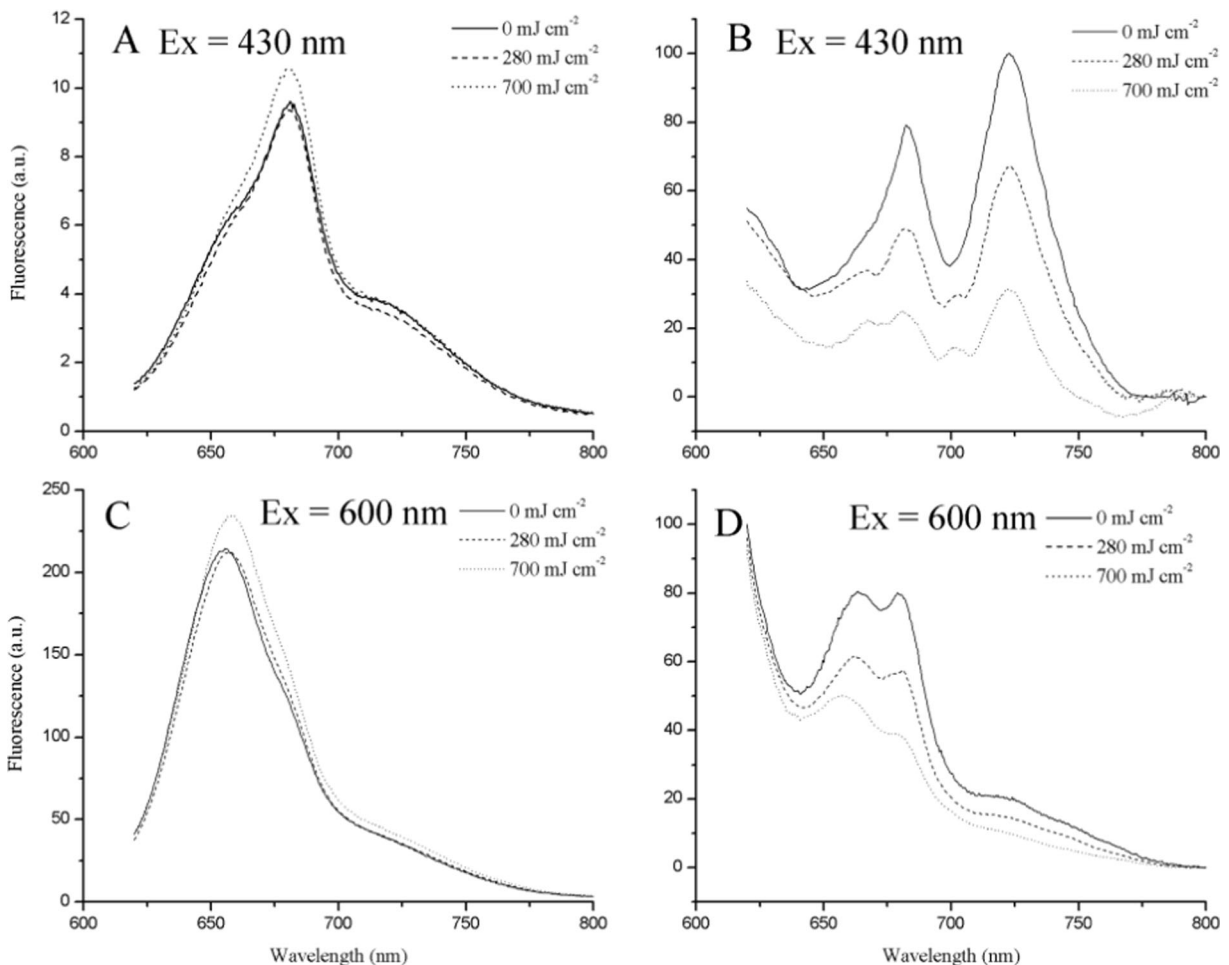


Fig. 2 Variations in fluorescence emission spectra of *M. aeruginosa* immediately after UV-C irradiation. The fluorescence emission spectra of healthy cells, 280 mJ cm^{-2} and 700 mJ cm^{-2} UV-C-treated cells were presented in *solid line*, *dashed line* and *dotted line*, respectively. **a** and **c** 288 K fluorescence emission

spectra at excitation of 430 and 600 nm, respectively, **b** and **d** 77-K fluorescence emission spectra at excitation of 430 and 600 nm, respectively. The 77-K absorbance spectra were normalized to the absorbance at 800 nm. Each curve was the mean of three replicates. The cell concentrations were at $5\text{-}\mu\text{g chlorophyll-a mL}^{-1}$

slight damage of photosynthetic apparatus followed by a recovery. Furthermore, the decreases of fluorescence emission spectra in Fig. 3e, f implied the decomposition of PS I, PS II, and PBS after 700-mJ cm^{-2} UV-C irradiation. The fluorescent bands were absent after 6-day cultivation, representing the irreversible impairment of photosynthetic apparatus.

3.3 Gene Expression

The results of *psbA* and *cpc* expressions are presented in Fig. 4. At 0 day, UV-C exposures resulted in a decrease of both *psbA* and *cpc* expressions. During the cultivation, the *psbA* expressions of the irradiated samples at 70 and 140 mJ cm^{-2} were significantly increased to 164 and 106 % of the control level at 4 days, respectively. The *psbA* expressions of the irradiated samples with more than 140 mJ cm^{-2} maintained lower than the control level during the cultivation. For *cpc* expression, a slight recover was observed in the irradiated samples at 70 and 140 mJ cm^{-2} . In contrast, no significant increase was observed in the *cpc* expressions of samples treated by higher dose UV-C irradiation.

3.4 TEM

The TEM images of control and treated *M. aeruginosa* cells are shown in Fig. 5. Figure 5a, b demonstrated a typical elliptical *M. aeruginosa* healthy cell (control sample) containing cell wall, cell membrane, thylakoids, and other cytoplasmic inclusion bodies. The cell wall tightly bonded cell membrane (circle A in Fig. 5b), indicating that this cell was intact and in an electrolyte balance condition. The cytoplasmic inclusions had regular structures and distributions, especially with the intact photosynthetic apparatus thylakoids (circle B) that ran in parallel or perpendicular to the cytoplasmic membrane and surrounded the entire cell area. Of note, hemispherically shaped PBS (arrows in Fig. 5b) attached to thylakoids was observed, demonstrating the typical light-harvesting antenna apparatus PBS in *M. aeruginosa* cells.

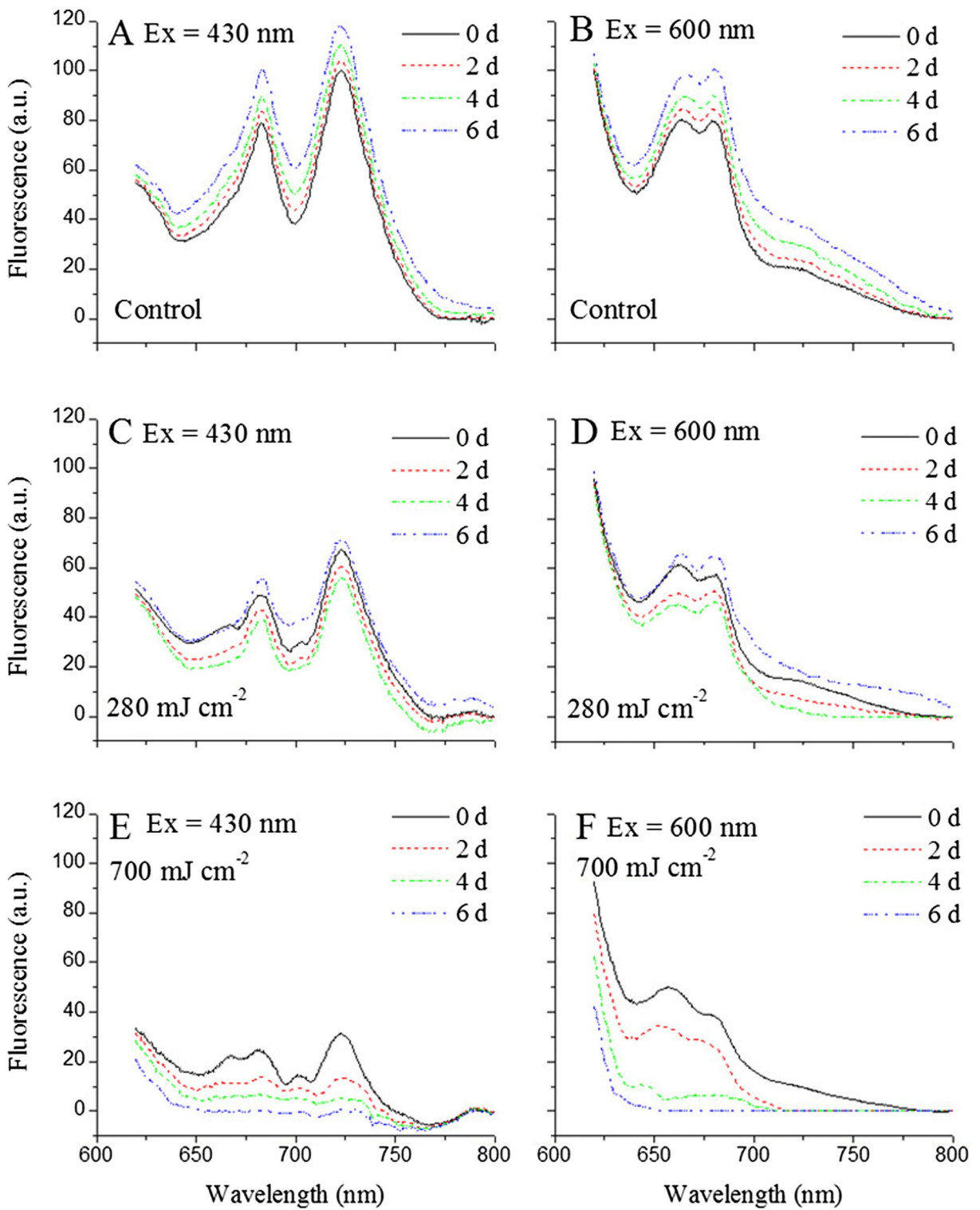
The cells under 700 and 4200 mJ cm^{-2} UV-C irradiation are shown in Figs. 4d and 5c. Two high-resolution images of another cell under 1400 mJ cm^{-2} irradiation are shown in Fig. 5e, f. After 700 mJ cm^{-2} UV-C radiation, the *M. aeruginosa* cells underwent damage (Fig. 5c). Two cavity areas were noticed (marked with circle), which demonstrated the intracellular damage of cytoplasmic inclusions. More severe damage was seen in the cells after

Fig. 3 Variations in fluorescence emission spectra of *M. aeruginosa* during cultivation after designed dosages UV-C irradiation. **a** and **b** 77-K fluorescence emission spectra of control sample at excitation of 430 and 600 nm, respectively, **c** and **d** 77-K fluorescence emission spectra of 280 mJ cm^{-2} UV-C treated sample at excitation of 430 and 600 nm, respectively, **e** and **f** 77-K fluorescence emission spectra of 700 mJ cm^{-2} UV-C treated sample at excitation of 430 and 600 nm, respectively. The absorbance spectra were normalized to the absorbance at 800 nm. Each curve was the mean of three replicates. The cell concentrations were at $5\text{-}\mu\text{g chlorophyll-a mL}^{-1}$

1400 mJ cm^{-2} UV-C (Fig. 5e). The drastic distortions of cell wall, including shrinking and wrinkling (arrow A) and a more significant cavity (circle), were observed. The hemispherically shaped PBS was absent in the lumen between two layers of thylakoids (arrow B). Moreover, other cytoplasmic inclusions, e.g., thylakoids membrane, exhibited irregular structures and distributions (arrow C). Similar damage in another cell was observed in Fig. 5f. The impairment of PBS and thylakoids indicated the destruction of photosynthetic apparatus.

3.5 Variations of LIC

Figure 6 presents the LIC of control and UV-C-treated samples at room temperature. State transition and non-photochemical quenching, which can be monitored by LIC, were used as indicators of photosynthetic capacities. Dark-adapted control sample presented low F_o and F_{md} values at 640 and 1060 a.u., respectively (Fig. 6a and Table 1). After illumination was shifted to a low-intensity white light, the stable fluorescence level (F_s) rose to 754 a.u. accompanied with the maximum F_m' value at 1248 a.u. The increase of fluorescence yield from 640 a.u. (F_o) to 754 a.u. (F_s) reflected a state transition (named as level 1 state transition) (Li et al. 2004), which was calculated by Eq. 2. The high Level 1 dF_s (105 a.u.) in control sample implied an excellent photoacclimation capacity in healthy cells. Subsequently, exposure of cells to a high-intensity white light-induced distinct variations of fluorescence yield. F_s increased from 754 to 898 a.u. (F_s'), and F_m' decreased from 1248 to 1130 a.u. (F_m''). The increase of F_s to F_s' reflected a further state transition (level 2 state transition), which can be calculated by Eq. 3. The decrease from F_m' to F_m'' indicated a capacity of non-photochemical quenching (Kirilovsky 2007), which can be calculated by Eq. 4. Significant non-photochemical quenching ($dF_m' = 121\text{ a.u.}$) and level 2 state transition (Level 2 $dF_s = 206\text{ a.u.}$) were observed in control samples during



saturating light illumination, suggesting the high efficiency of photoprotection.

The LIC of UV-C-treated samples are presented in Fig. 6b–e. Compared with control sample ($F_o=640$ a.u.), F_o went up to 760 and 1045 a.u., respectively, after 140 and 1400 mJ cm^{-2} UV-C treatments (Table 1). The Level 1 dF_s decreased from 86 to 65 a.u. when the UV-C dosage increased from 140 to 700 mJ cm^{-2} ; then it dramatically declined to 28 a.u. when the UV-C dosage reached 1400 mJ cm^{-2} . Furthermore, the Level 2 dF_s and dF_m'

gradually decreased from 206 to 4 a.u. and from 121 to 10 a.u., respectively, when the UV-C dosage increased from 0 to 1400 mJ cm^{-2} .

3.6 Variations of Cell Density

Irreversible impairment of photosynthesis induced failure of reproduction and growth of *M. aeruginosa* cells. The variations of cell density are shown in Fig. 7. The cell density of control sample gradually increased from

Fig. 4 Effects of UV-C irradiation on *psbA* and *cpc* gene expression of *M. aeruginosa*. Each column was the mean of three replicates

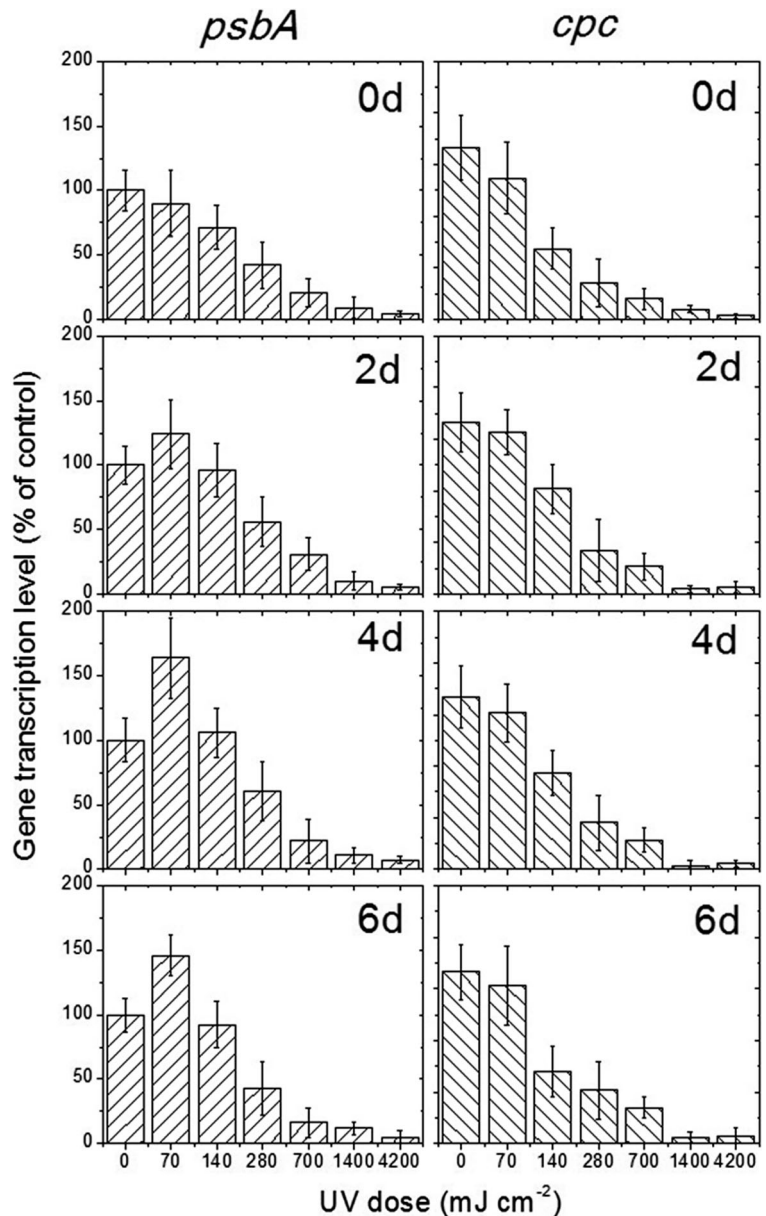
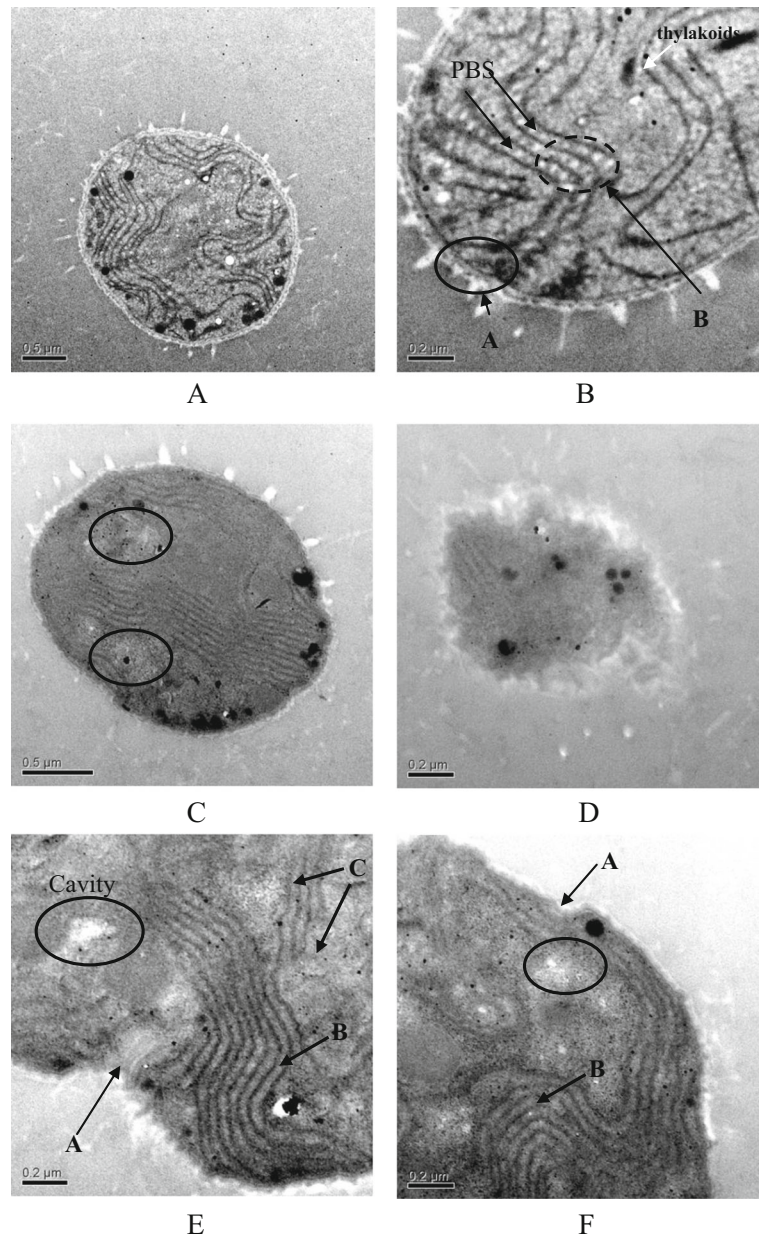


Fig. 5 TEM ultrastructure images of control and UV-C treated *M. aeruginosa* cells. **a** and **b** control cells in 40000 \times and 80000 \times resolution ratio, **c** and **d** cells under 700 and 4200 mJ cm⁻² UV-C radiation in 40000 \times resolution ratio, **e** and **f** cells under 1400 mJ cm⁻² UV-C radiation in 80000 \times resolution ratio



4.6×10^6 to 9.1×10^6 cells mL⁻¹ within 6 days. The cell density increased from 4.6×10^6 to 5.8×10^6 cells mL⁻¹ after 140 mJ cm⁻² UV-C irradiation. After 280 mJ cm⁻² UV-C, the cell density decreased from 4.5×10^6 to 2.8×10^6 cells mL⁻¹ in initial 4 days; then it increased to 4.1×10^6 cells mL⁻¹ in the subsequent 2-day cultivation. The cell density of 700 mJ cm⁻²-treated sample decreased to 0.1×10^6 cells mL⁻¹ at 4 days, and no recovery was observed. Similar phenomena were observed in higher dosages UV-C-treated samples.

4 Discussion

4.1 Degradation of Photosynthetic Pigments

The result of TCC indicated that > 280 mJ cm⁻² UV-C induced a decrease of chlorophyll-a (Fig. 1a), which was in agreement with our previous study (Ou et al. 2011). UV-C can induce decomposition of photosynthetic pigments in cyanobacteria. Of note, the transitory increase of MCC during the cultivation after 70–700 mJ cm⁻²

UV-C treatment demonstrated an accumulation of pigments. This phenomenon may be a response to screen out UV-C irradiation that was induced by UV-C stress. Degradation of chlorophyll-a was observed after higher dosage UV-C irradiation (Fig. 1a, 4200 mJ cm^{-2}). The suppression of *cpc* gene expression was also observed (Fig. 4), suggesting a damage of DNA and transcription of PC. Since chlorophyll-a and PC are the key pigments in PS I, PS II, and PBS, the degradation of them may result in critical damage of photosynthetic apparatus, resulting in a failure of light absorption.

4.2 Decomposition of Photosynthetic Apparatus

The 77-K fluorescence emission spectra of subunits (CP43 at 685 nm and CP47 at 695 nm) in PS II/PS I and subunits (PC at 650 nm and APC at 660 nm) in PBS all decreased after 700 mJ cm^{-2} UV-C irradiation (Figs. 2 and 3). Furthermore, incomplete PBS and thylakoids membrane were observed in the TEM images after UV-C irradiation (Fig. 5, 700 mJ cm^{-2}). The decrease of *pbsA* gene expression was also observed (Fig. 4), indicating a suppression of the D1 protein transcription after UV-C irradiation. These results represented the UV-C-induced damage of the photosynthetic apparatus, including PS II, PS I, PBS, and thylakoids membrane. These apparatus play important roles in photosynthesis. Illumination can be efficiently absorbed by PBS, then the energy is transferred into PS II and PS I. In cyanobacteria, the primary reaction of photosynthesis is performed in this system associated with other principal metabolic paths, and it is indispensable for energy and mass supply. The impairment of these photosynthetic apparatus can induce failure of photosynthesis.

4.3 Inhibition of Photoacclimation and Photoprotection

State transition and non-photochemical quenching were two important physiological phenomena in cyanobacteria (Mullineaux and Emlyn-Jones 2005; Rakhimberdieva et al. 2004). The LIC results indicated that UV-C induced significant inhibition of these two phenomena (Fig. 6). State transition was believed to be an accommodation strategy that regulated the relative energy transfer from PBS to PS I/PS II in cyanobacteria (Kirilovsky 2007). Two physiological functions of state transition

Fig. 6 Light-induced curves of *M. aeruginosa* after UV-C irradiation. Changes in fluorescence levels induced by different intensities of white light measured by a PAM. **a** Dark-adapted control *M. aeruginosa* cells ($5\text{-}\mu\text{g}$ chlorophyll-a mL^{-1}) was successively illuminated with white light at $60 \mu\text{mol photons m}^{-2} \text{ s}^{-1}$ followed by white light at $600 \mu\text{mol photons m}^{-2} \text{ s}^{-1}$. Saturating pulses (0.5-s duration, $2000 \mu\text{mol photons m}^{-2} \text{ s}^{-1}$) were applied to measure F_{m} and F_{m}' values in darkness and in actinic light, respectively. **b–e** UV-C-treated *M. aeruginosa* cells were also illuminated follow the same sequence of light. The UV-C irradiated dose of sub-image B-E were 140, 280, 700, and 1400 mJ cm^{-2} , respectively

were confirmed in the previous studies, including the optimization of energy harvesting under low intensity illumination (a type of photoacclimation) (Mullineaux and Emlyn-Jones 2005) and the re-configuration of excess energy under intense illumination (a type of photoprotection) (Ma et al. 2007). Level 1 and 2 state transitions mentioned in section “Variations of LIC” may represent the photoacclimation and photoprotection, respectively. Compared with the decrease of Level 1 dF_{s} (from 105 a.u. to 65 a.u., after 700 mJ cm^{-2} irradiation), the decrease of Level 2 dF_{s} (from 206 a.u. to 35 a.u., after 700 mJ cm^{-2} irradiation) was faster (Table 1). This result implied UV-C preferentially impaired the photoprotection capacity but not the photoacclimation function; however, both functions were critically suppressed by higher dosage UV-C (1400 mJ cm^{-2}).

The non-photochemical quenching also reflects the capacity of photoprotection, which was represented by dF_{m}' in the current study. The dF_{m}' decreased from 121 to 23 a.u. after 140 mJ cm^{-2} UV-C irradiation (Table 1), suggesting that the non-photochemical quenching capacity was inhibited by UV-C. According to the previous studies (Rakhimberdieva et al. 2004; Scott et al. 2006; Wilson et al. 2006), the quenching of F_{m}' in LIC was an energy dissipation process related to PBS and APC-orange carotenoid protein (OCP) complex, accompanied with the decrease of fluorescence emission from PBS. Intact APC and OCP are essential to this non-photochemical quenching under excess illumination (Gorbunov et al. 2011). Moreover, PS I, PS II, and membrane lipids were proposed to be the potential participants for this non-photochemical quenching process (Karapetyan 2007; Rakhimberdieva et al. 2007). All these apparatus were ruined by UV-C (Fig. 2b and d), resulting in a suppression of non-photochemical quenching (dF_{m}').

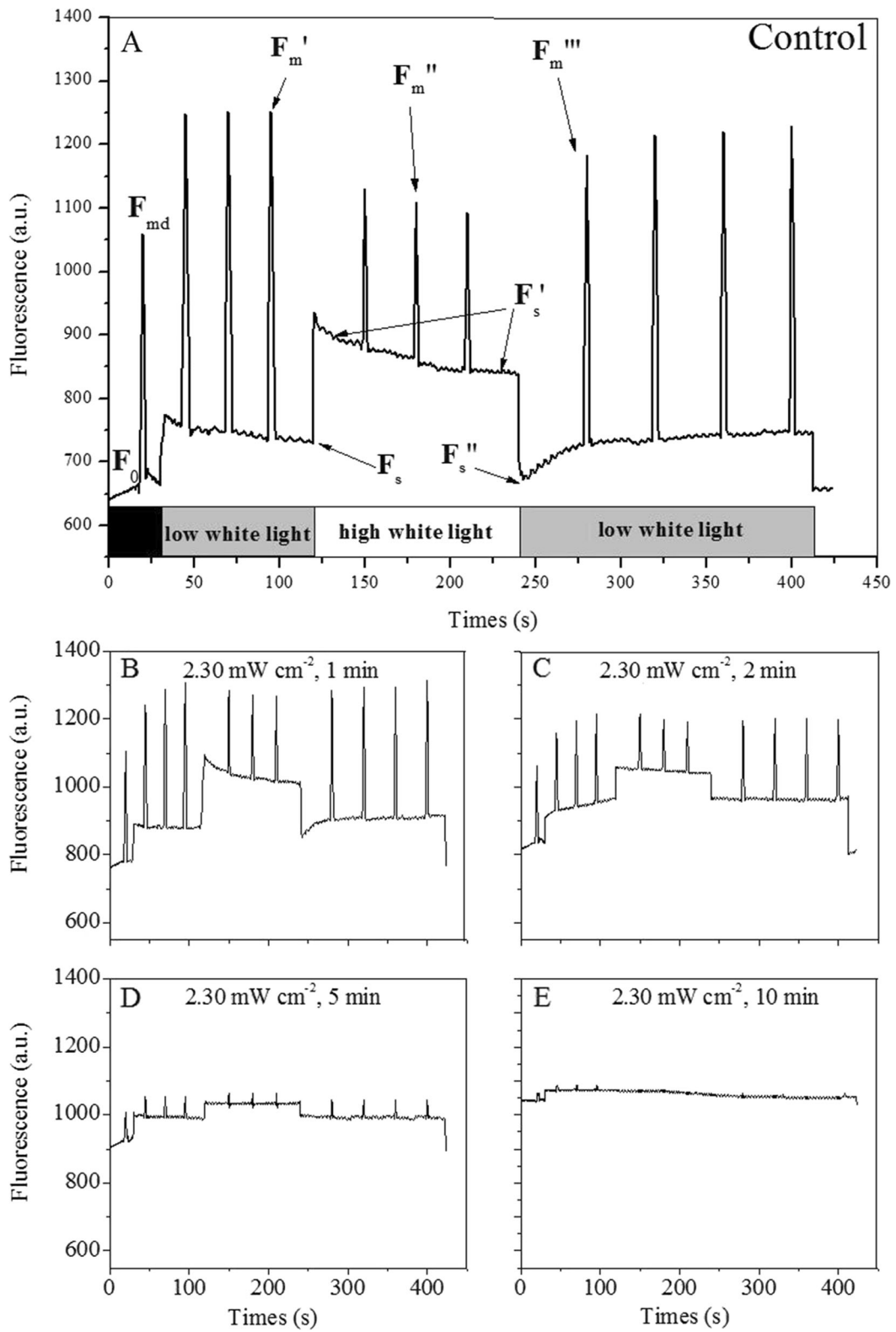


Table 1 Original fluorescence parameters of light induced curves of *M. aeruginosa* after UV-C irradiation

UV-C dosage (mJ cm ⁻²)	Initial F _o (a.u. ^a)	Level 1 dF _s (a.u. ^a)	Level 2 dF _s (a.u. ^a)	dF _m ' (a.u. ^a)
0	640	105	206	121
140	760	86	205	23
280	814	85	85	19
700	902	65	35	14
1400	1045	28	4	10

Level 1 dF_s and Level 2 dF_s present the level 1 and level 2 state transitions, respectively, and the dF_m' demonstrates the capacity of non-photochemical quenching

^a The unit of fluorescence parameters is a.u.

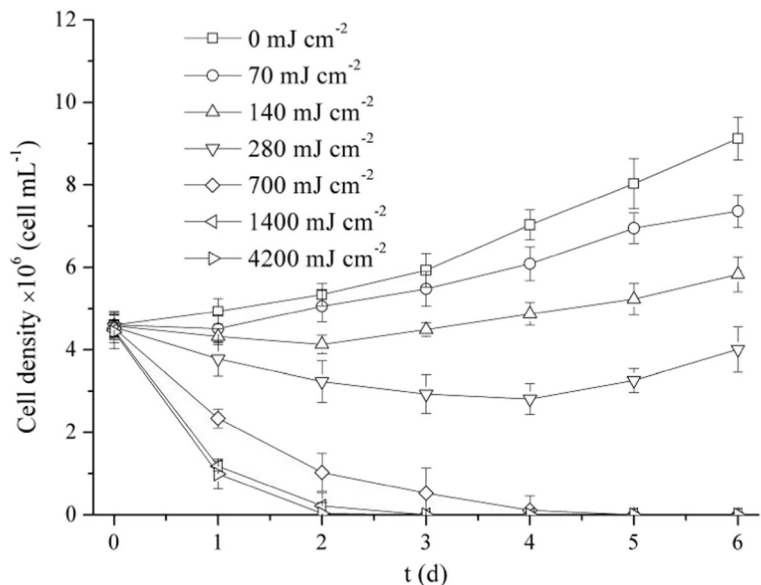
4.4 Death of *M. aeruginosa* Cell

After UV-C irradiation, the cell colony theoretically can be divided into two parts according to the damage levels of photosynthesis. The first part of cells had received relatively slight and reversible damage on photosynthesis. In these cells, the impaired photosynthetic pigments and apparatus were repaired during the cultivation after UV-C. Furthermore, the impaired genetic system was also repaired, finally resulting in a recovering. The result of *pbsA* and *cpc* expressions in cultivation also confirmed the recovery of genetic system of the samples treated by a low-dose UV-C irradiation (70–140 mJ cm⁻²). According to previous research, this phenomenon may be identified as photoreactivation

repair (Sakai et al. 2011). To the contrary, the second part of cells had suffered irreversible damage on the photosynthetic pigments and apparatus. Without intact apparatus, the light harvesting and energy transferring of photosynthesis were cut off. Furthermore, photoacclimation and photoprotection were completely deprived by UV-C. Therefore, the second part of cells will suffer further impairments from illumination during cultivation, finally resulting in death.

The proportions of these two parts of cells depended on the UV-C irradiation dosages. And their variations induced changes of cell density (Fig. 7). Under lower-dosages UV-C (140 and 280 mJ cm⁻²), the first part was the majority in colony. The minority second part of cells died in initial 2–3-day cultivation, resulting in the decreases of cell density. For example, the cell density decreased from 4.6×10^6 to 4.1×10^6 cells mL⁻¹ after 140 mJ cm⁻² irradiation (Fig. 7). The growth and reproduction of the first part of cells resulted in continuous increase of cell biomass from 4 to 6 days. The cell density increased from 4.1×10^6 to 5.8×10^6 cells mL⁻¹ after 140 mJ cm⁻² irradiation (Fig. 7). To the contrary, the second part of cells was the majority in the colony under higher dosages UV-C (700–4200 mJ cm⁻²). The cell density decreased to 0 at 4 days under these dosages UV-C (Fig. 7), implied all cells suffered irreversible impairment. The recovery and dying processes of cells lasted for several hours or days, which depended on the UV-C irradiation dosages. For example, the cell density decreased from 4.5×10^6 cells

Fig. 7 Variations of *M. aeruginosa* cell density during cultivation after UV-C irradiation. Cells were exposed to designated dosages UV-C irradiation before cultivated experiments. Data were the means of three independent samples; error bars indicated the ± 1 standard deviation of each data set



mL^{-1} (0 day) to 0.5×10^6 cells mL^{-1} (3 days); then it decreased to 0 (4 days) after 700 mJ cm^{-2} UV-C irradiation. In the case of 1400 mJ cm^{-2} , the cell density decreased to 0.2×10^6 cells mL^{-1} at 2 days and 0 at 3 days, indicating that higher dosage UV-C induced rapid decomposition of cells. Furthermore, the complete inactivation within 4-day cultivation ($>280 \text{ mJ cm}^{-2}$ UV-C) suggested that there would be a UV-C dosage threshold region ($280\text{--}700 \text{ mJ cm}^{-2}$) to induce the complete inactivation of given biomass ($\sim 4.6 \times 10^6$ cells mL^{-1}) *M. aeruginosa* suspension.

5 Conclusions

In the current study, the UV-C-induced impairment on photosynthetic system of *M. aeruginosa* can be summarized as a three steps process: (1) degradation of photosynthetic pigments, (2) decomposition of photosynthetic apparatus, and (3) inhibition of photoacclimation and photoprotection. These impairments resulted in a decline of cyanobacteria biomass, which depended on the UV-C irradiation dosage. For 4.6×10^6 cells mL^{-1} *M. aeruginosa*, a $700\text{--}4200 \text{ mJ cm}^{-2}$ UV-C irradiation caused a continuous decrease of cell density (from 4.5×10^6 cells mL^{-1} to 0) within 6-day cultivation. These results suggested that there was an optimal UV-C dosage threshold to inactivate all the cells with a given cyanobacteria biomass. The determination of this threshold would improve the removal efficiency and save the energy cost for the cyanobacteria removal using UV-C irradiation in water treatment.

Acknowledgments This project was supported by the National Natural Science Foundation of China (grant no. 51308224), the Science and Technology Planning Project of Guangdong Province, China (grant no. 2014A020216014), and the State Key Program of the National Natural Science Foundation of China (grant no. 21037001).

References

- Azevedo, S. M. F. O., Carmichael, W. W., Jochimsen, E. M., Rinehart, K. L., Lau, S., Shaw, G. R., & Eaglesham, G. K. (2001). Human intoxication by microcystins during renal dialysis treatment in Caruaru-Brazil. *Toxicology*, *164*, 32–32.
- Bailey, S., & Grossman, A. (2008). Photoprotection in cyanobacteria: regulation of light harvesting. *Photochemistry and Photobiology*, *84*, 1410–1420.
- Boulay, C., Abasova, L., Six, C., Vass, I., & Kirilovsky, D. (2008). Occurrence and function of the orange carotenoid protein in photoprotective mechanisms in various cyanobacteria. *BBA-Bioenergetics*, *1777*, 1344–1354.
- Briand, J. F., Jacquet, S., Bernard, C., & Humbert, J. F. (2003). Health hazards for terrestrial vertebrates from toxic cyanobacteria in surface water ecosystems. *Veterinary Research*, *34*, 361–377.
- Campbell, D., Hurry, V., Clarke, A. K., Gustafsson, P., & Oquist, G. (1998). Chlorophyll fluorescence analysis of cyanobacterial photosynthesis and acclimation. *Microbiology and Molecular Biology Reviews*, *62*, 667–683.
- Chen, L. Z., Xie, M., Bi, Y. H., Wang, G. H., Deng, S. Q., & Liu, Y. D. (2012). The combined effects of UV-B radiation and herbicides on photosynthesis, antioxidant enzymes and DNA damage in two bloom-forming cyanobacteria. *Ecotoxicology and Environmental Safety*, *80*, 224–230.
- de Figueiredo, D. R., Azeiteiro, U. M., Esteves, S. M., Goncalves, F. J. M., & Pereira, M. J. (2004). Microcystin-producing blooms—a serious global public health issue. *Ecotoxicology and Environmental Safety*, *59*, 151–163.
- Gorbunov, M. Y., Kuzminov, F. I., Fadeev, V. V., Kim, J. D., & Falkowski, P. G. (2011). A kinetic model of non-photochemical quenching in cyanobacteria. *BBA-Bioenergetics*, *1807*, 1591–1599.
- He, Y. Y., & Hader, D. P. (2002). Reactive oxygen species and UV-B: effect on cyanobacteria. *Photochemical and Photobiological Sciences*, *1*, 729–736.
- Huang, J., Graham, N., Templeton, M. R., Zhang, Y., Collins, C., & Nieuwenhuijsen, M. (2009). A comparison of the role of two blue-green algae in THM and HAA formation. *Water Research*, *43*, 3009–3018.
- Karapetyan, N. V. (2007). Non-photochemical quenching of fluorescence in cyanobacteria. *Biochemistry (Moscow)*, *72*, 1127–1135.
- Kirilovsky, D. (2007). Photoprotection in cyanobacteria: the orange carotenoid protein (OCP)-related non-photochemical-quenching mechanism. *Photosynthesis Research*, *93*, 7–16.
- Li, D. H., Xie, J., Zhao, J. Q., Xia, A. D., Li, D. H., & Gong, Y. D. (2004). Light-induced excitation energy redistribution in *Spirulina platensis* cells: “spillover” or “mobile PBSs”? *BBA-Bioenergetics*, *1608*, 114–121.
- Li, X., Zhao, Q., Zhou, W., Xu, L., & Wang, Y. (2015). Effects of chronic exposure to microcystin-LR on hepatocyte mitochondrial DNA replication in mice. *Environmental Science & Technology*, *49*.
- Lu, F., Wang, G. C., & Jin, H. C. (2011). Photosynthetic responses of thalli and isolated protoplasts of *Bryopsis hypnoides* (Bryopsidales, Chlorophyta) during dehydration. *Chinese Journal of Oceanology and Limnology*, *29*, 334–342.
- Ma, W. M., Ogawa, T., Shen, Y. G., & Mi, H. L. (2007). Changes in cyclic and respiratory electron transport by the movement of phycobilisomes in the cyanobacterium *Synechocystis* sp strain PCC 6803. *BBA-Bioenergetics*, *1767*, 742–749.
- MacColl, R. (1998). Cyanobacterial phycobilisomes. *Journal of Structural Biology*, *124*, 311–334.
- Mullineaux, C. W., & Emlin-Jones, D. (2005). State transitions: an example of acclimation to low-light stress. *Journal of Experimental Botany*, *56*, 389–393.
- Nield, J., Morris, E. P., Bibby, T. S., & Barber, J. (2003). Structural analysis of the photosystem I supercomplex of cyanobacteria

- induced by iron deficiency. *Biochemistry-US*, 42, 3180–3188.
- Ou, H. S., Gao, N. Y., Deng, Y., Qiao, J. L., Zhang, K. J., Li, T., & Dong, L. (2011). Mechanistic studies of *Microcystis aeruginosa* inactivation and degradation by UV-C irradiation and chlorination with poly-synchronous analyses. *Desalination*, 272, 107–119.
- Ou, H., Gao, N. Y., Deng, Y., Qiao, J. L., & Wang, H. (2012). Immediate and long-term impacts of UV-C irradiation on photosynthetic capacity, survival and microcystin-LR release risk of *Microcystis aeruginosa*. *Water Research*, 46, 1241–1250.
- Parmar, A., Singh, N. K., Pandey, A., Gnansounou, E., & Madamwar, D. (2011). Cyanobacteria and microalgae: a positive prospect for biofuels. *Bioresource Technology*, 102, 10163–10172.
- Rakhimberdieva, M. G., Stadnichuk, I. N., Elanskaya, T. V., & Karapetyan, N. V. (2004). Carotenoid-induced quenching of the phycobilisome fluorescence in Photosystem II-deficient mutant of *Synechocystis* sp. *FEBS Letters*, 574, 85–88.
- Rakhimberdieva, M. G., Vavilin, D. V., Vermaas, W. F. J., Elanskaya, I. V., & Karapetyan, N. V. (2007). Phycobilin/chlorophyll excitation equilibration upon carotenoid-induced non-photochemical fluorescence quenching in phycobilisomes of the *Synechocystis* sp PCC 6803. *BBA-Bioenergetics*, 1767, 757–765.
- Ralph, P. J., & Gademann, R. (2005). Rapid light curves: a powerful tool to assess photosynthetic activity. *Aquatic Botany*, 82, 222–237.
- Sakai, H., Katayama, H., Oguma, K., & Ohgaki, S. (2011). Effect of photoreactivation on ultraviolet inactivation of *Microcystis aeruginosa*. *Water Science and Technology*, 63, 1224–1229.
- Scott, M., McCollum, C., Vasil'ev, S., Crozier, C., Espie, G. S., Krol, M., Huner, N. P. A., & Bruce, D. (2006). Mechanism of the down regulation of photosynthesis by blue light in the cyanobacterium *Synechocystis* sp PCC 6803. *Biochemistry-US*, 45, 8952–8958.
- Vaishampayan, A., Sinha, R. P., Hader, D. P., Dey, T., Gupta, A. K., Bhan, U., & Rao, A. L. (2001). Cyanobacterial biofertilizers in rice agriculture. *Botanical Review*, 67, 453–516.
- Watson, S. B., Ridal, J., & Boyer, G. L. (2008). Taste and odour and cyanobacterial toxins: impairment, prediction, and management in the great lakes. *Canadian Journal of Fisheries and Aquatic Sciences*, 65, 1779–1796.
- White, A. J., & Critchley, C. (1999). Rapid light curves: a new fluorescence method to assess the state of the photosynthetic apparatus. *Photosynthesis Research*, 59, 63–72.
- Wilson, A., Ajlani, G., Verbavatz, J. M., Vass, I., Kerfeld, C. A., & Kirilovsky, D. (2006). A soluble carotenoid protein involved in phycobilisome-related energy dissipation in cyanobacteria. *Plant Cell*, 18, 992–1007.
- Wilson, A., Boulay, C., Wilde, A., Kerfeld, C. A., & Kirilovsky, D. (2007). Light-induced energy dissipation in iron-starved cyanobacteria: roles of OCP and IsiA proteins. *Plant Cell*, 19, 656–672.
- Yi, T., Xianzhong, M., Jiangyong, H., Mok, H. O. L., Lingyun, W., Au, D. W. T., Jia, Z., & Xihui, Z. (2013). Mechanisms of photosynthetic inactivation on growth suppression of *Microcystis aeruginosa* under UV-C stress. *Chemosphere*, 93, 637–644.
- Zhou, H., & Smith, D. W. (2001). Advanced technologies in water and wastewater treatment. *Canadian Journal of Civil Engineering*, 28, 49–66.